# RAPID COMMUNICATION

# Cs$_2$CuP$_3$S$_9$: A Chiral Compound with Screw Helices

Jason A. Hanko and Mercouri G. Kanatzidis[1]

*Department of Chemistry and Center for Fundamental Materials Research, Michigan State University, East Lansing, Michigan 48824*

The reaction of Cu with a molten mixture of Cs$_2$S/P$_2$S$_5$ produced the quaternary compound Cs$_2$CuP$_3$S$_9$. The bright yellow crystals of Cs$_2$CuP$_3$S$_9$ are stable in air and water for several weeks. The compound crystallizes in the chiral, hexagonal space group $P6_5$ (No. 170) and at 23°C: $a = 15.874(2)$ Å; $c = 35.100(7)$ Å; $V = 7660(3)$ Å$^3$; $Z = 18$. The [CuP$_3$S$_9$]$_n^{2n-}$ chains are composed of an alternating arrangement of tetrahedral Cu$^+$ ions and cyclic [P$_3$S$_9$]$^{3-}$ units. The structure contains parallel helical [CuP$_3$S$_9$]$_n^{2n-}$ chains that run along the $c$-axis. The cyclic [P$_3$S$_9$]$^{3-}$ unit derives from the molecular adamantane [P$_4$S$_{10}$] unit with one [PS]$^{3+}$ vertex removed. The title compound was characterized by differential thermal analysis, far-IR, Raman, and single-crystal optical transmission UV/vis spectroscopy. Positive nonlinear optical response and second harmonic generation response was observed. © 2000 Academic Press

## INTRODUCTION

The use of chalcophosphate fluxes has enabled the discovery of many new chalcophosphate compounds (1). These fluxes are commonly formed by the *in situ* fusion of $A_2Q$/P$_2Q_5$/$Q$ ($A$ = alkali metal; $Q$ = S, Se), forming a variety of [P$_yQ_z$]$^{n-}$ units in a molten polychalcogenide solvent. In these "solutions" metals are oxidized and then "captured" by the various [P$_yQ_z$]$^{n-}$ units, building up extended frameworks which, if anionic, are stabilized by alkali cations. This approach has produced several unusual compounds; examples include Cs$_2M_2$P$_2$Se$_6$ ($M$ = Cu, Ag) (2), K$_3M_3$P$_3$Se$_9$ ($M$ = Cu (3), Ag (4)), $A$La(P$_2$Se$_6$) (5), the mixed-valent $A_6$Au$_{1.5}^I$Au$_{1.5}^{III}$(P$_2$Se$_6$)$_3$ ($A$ = K, Rb) (6), $A_3$AuP$_2$Se$_8$ ($A$ = K, Rb, Cs) (7), $A_2$Au$_2$P$_2$Se$_6$ ($A$ = K, Rb) (7), $A_2$AuPS$_4$ ($A$ = K, Rb, Cs) (7), $A$AuP$_2$S$_7$ ($A$ = K, Rb) (7), K$_3$CuP$_2$S$_7$ (8), $A_2$CuP$_3$S$_9$ ($A$ = K, Rb) (8), Cs$_2$Cu$_2$P$_2$S$_6$ (8), Rb$_4$Sn$_2$Ag$_4$(P$_2$Se$_6$)$_3$ (9), K$_2$Cu$_2$P$_4$Se$_{10}$ (10), [Cr$_2$(PS$_4$)$_4$] (6–11), and CsTa$_4$S$_5$(S$_2$)(PS$_4$)$_3$ (12). One of the lessons

learned from these studies, for example, is that increasing the concentration of P$_2$S$_5$ in the flux favors the formation of higher order species such as [P$_2$S$_7$]$^{4-}$ and the cyclic
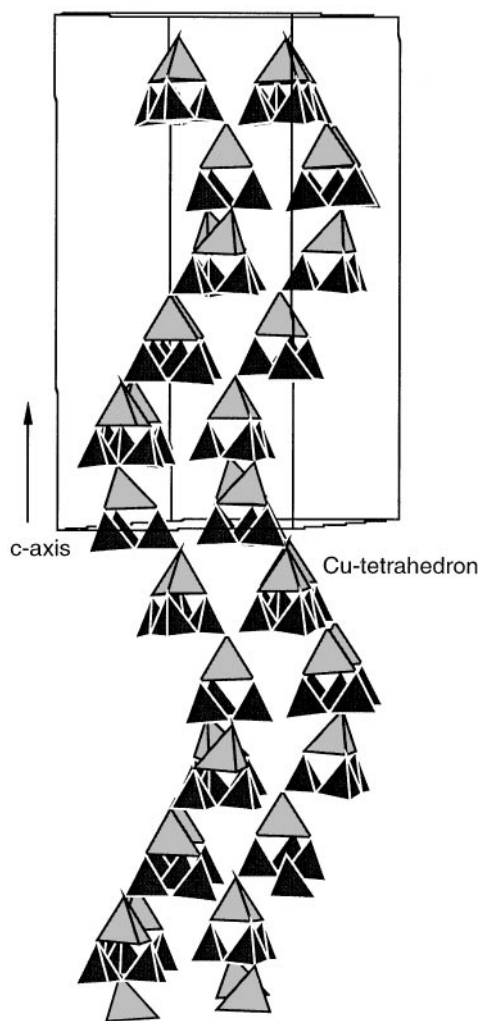


**FIG. 1.** ORTEP representation of Cs$_2$CuP$_3$S$_9$ as viewed perpendicular to the $c$-axis (50% probability ellipsoids). Ellipsoids with octant shading are Cu atoms, boundary and axis ellipsoids are P atoms, boundary ellipsoids are S, and principal and axis ellipsoids are Cs atoms.

---

[1]To whom correspondence should be addressed.

$[P_3S_9]^{4-}$ units, whereas increasing the concentration of $A_2S$ tends to break down those species and stabilize the discrete and fundamental $[PS_4]^{3-}$ unit. In the context of these investigations we have discovered $Cs_2CuP_3S_9$ (**I**), a hexagonal *chiral* compound with helical screw chains of $[CuP_3S_9]^{2-}$ conforming to a $6_5$ screw axis (13). *Discrete*



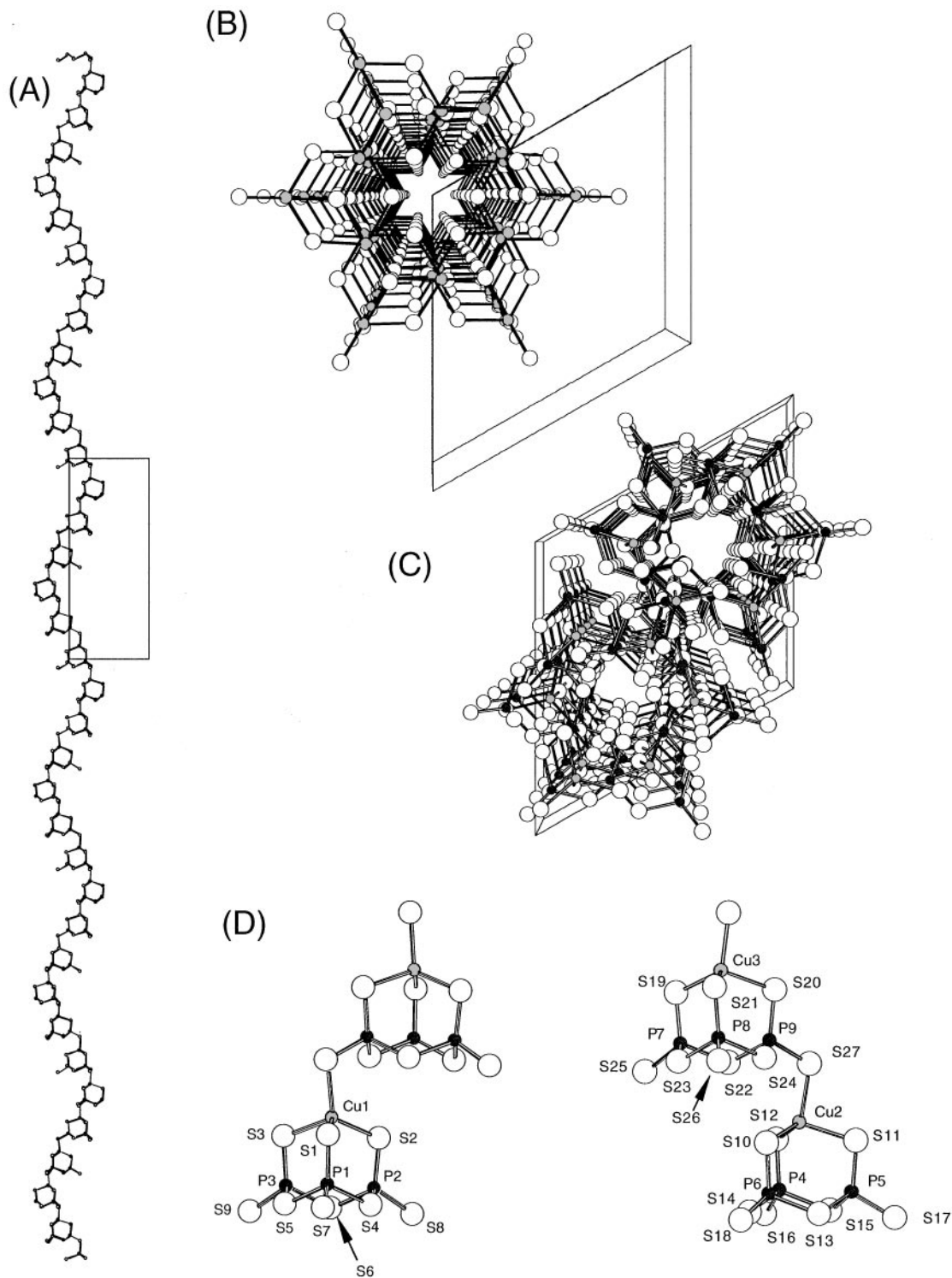**FIG. 2.** (A) View of a long filament of the infinite $[CuP_3S_9]_n^{2n-}$ chain to show the helical conformation. (B) View down the helical axis of a $[CuP_3S_9]_n^{2n-}$ chain containing Cu(1). (C) View down the helical axis of a $[CuP_3S_9]_n^{2n-}$ chain containing Cu(2) and Cu(3). (D) Fragments from each chain showing the adamantane clusters and the atomic labeling scheme.

*chiral* inorganic helices crystallizing in polar space groups are rare with HgS and elemental Se and Te being examples.

The unit cell of $Cs_2CuP_3S_9$ (14) is shown in Fig. 1. A careful look reveals three independent helices running down the *c*-axis. They are composed of alternating cyclic $[P_3S_9]^{3-}$ units chelating in a tridendate fashion to $Cu^+$ ions; see Fig. 2. The binding to Cu ions leads to recognizable adamantane $[CuP_3S_{10}]$ clusters which propagate to form a helix by sharing two sulfur atoms. In all $[CuP_3S_9]_n^{2n-}$ helices in the crystal, all dipoles point in the same direction, giving rise to the $P6_5$ space group. The three parallel $[CuP_3S_9]_n^{2n-}$ chains in the cell are separated crystallographically into two different kinds: one which consists of a single chain containing Cu(1) propagates and coils around the *c*-axis itself, and another which consists of two identical helices with their axes located at 1/3, 1/3 and 2/3, 2/3, respectively. The latter contains the atoms Cu(2) and Cu(3). A view of the two types of $[CuP_3S_9]_n^{2n-}$ screw helix is shown in Figs. 2B and 2C. Using a threaded bolt analogy, we can describe the overall side-by-side packing of the helical chains such that the ridges of one fit in the grooves of its nearest neighbors. The average Cu–S distance of the three $[CuS_4]$ tetrahedra is 2.306(9), 2.307(9), and 2.316(7) Å for Cu(1), Cu(2), and Cu(3), respectively. The S–Cu–S angles display a slight distortion from the tetrahedral geometry, with an average S–Cu–S angle of 109(2)°, 109(1)°, and 109(2)° for Cu(1), Cu(2), and Cu(3), respectively.

The two $[CuP_3S_9]_n^{2n-}$ chains in (I) contain three crystallographically different $[P_3S_9]^{3-}$ units, with normal P–S bond distances in the range from 1.954(4) to 2.139(3) Å with an average P–S distance of 2.05(3) Å. The S–P–S angles reveal only slight distortions from the ideal tetrahedral coordination geometry, with an average angle of 109(2)°. The $[P_3S_9]^{3-}$ unit contains a cyclic $[P_3S_3]$ ring (chair conformation) with a mean P–P distance of 3.483(3) Å. There are two types of P–S distances in the three different cyclic $[P_3S_9]^{3-}$ units: the longer P–S distances within the $P_3S_3$ ring at 2.11(5) Å, and the shorter P–S distances for the terminal sulfide atoms at 1.97(1) Å.

The $[CuP_3S_9]_n^{2n-}$ chains are separated by $Cs^+$ ions that are located in six different sites. The coordination of the $Cs^+$ counterions is made of sulfur atoms and varies from 8 to 10. The *helical screw*-like, polar $[CuP_3S_9]_n^{2n-}$ chains in (I) differ dramatically from the *straight* chains of $A_2CuP_3S_9$ ($A$ = K, Rb) (8), which also pack in a centrosymmetric fashion.

The optical absorption properties of $Cs_2CuP_3S_9$ were assessed by measuring the optical transmission spectrum of single crystal samples; see Fig. 3A. The sharp optical gap observed in the spectrum indicates that the compound is a wide band-gap semiconductor with a gap $E_g \sim 2.4$ eV. Below the band-gap the material shows good optical transparency down to the infrared region up to 0.2 eV.

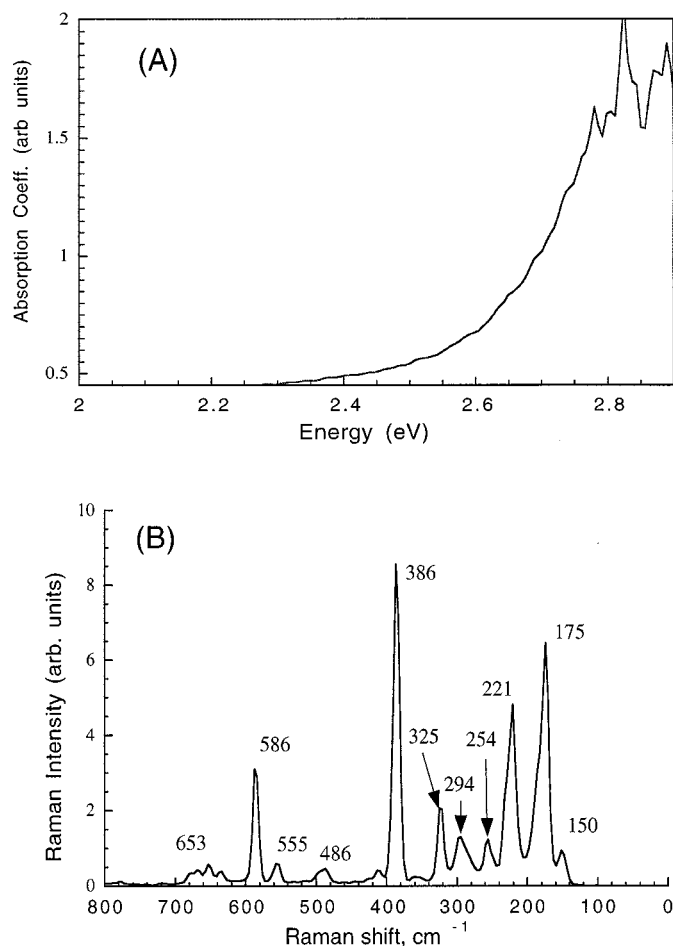The far-IR (15) spectrum of $Cs_2CuP_3S_9$ displays several absorptions in the 620–400 cm$^{-1}$ range. The sharp absorp-



**FIG. 3.** (A) Single-crystal optical absorption spectrum of $Cs_2CuP_3S_9$. The sharp features at high absorbance are noise and due to the very low transmission of light at those energies. (B) Raman spectrum of $Cs_2CuP_3S_9$.

tion at 400 and 463 cm$^{-1}$ are characteristic of the P–S–P stretching vibrations in the cyclic $[P_3S_9]^{3-}$ unit. The remaining absorptions are tentatively assigned to the $-PS_2$ stretching vibrations by analogy to $AAuP_2S_7$ ($A$ = K, Rb) (7). Absorptions below 400 cm$^{-1}$ are assigned to Cu–S stretching vibrations. The Raman spectrum (15) of $Cs_2CuP_3S_9$, shown in Fig. 3B, displays shifts in the 675- to 250-cm$^{-1}$ range that are tentatively assigned to P–S and shifts below 250 cm$^{-1}$ are assigned to Cu–S stretching vibrations. The shifts at ca. 386 and 294 cm$^{-1}$ are assigned to the $[PS_4]^{3-}$ by analogy to $A_2AuPS_4$, $A_2AuP_2S_7$ ($A$ = K, Rb) (7), and $A_2P_2S_6$ ($A$ = K, Cs) (16). The Raman spectrum of $Cs_2CuP_3S_9$ is shown in Fig. 3B. Differential thermal analysis followed by careful XRD analysis of the residues revealed that the title compound melts incongruently at $\sim 477$°C, forming a mixture of $Cs_2CuP_3S_9$ and $Cs_2P_2S_6$ (17) and a ternary Cu/P/S phase.

The unique chiral structure of $Cs_2CuP_3S_9$ is evidently stabilized by the Cs cation. The polar character makes the

compound a potential candidate for nonlinear optical applications. Preliminary qualitative tests for nonlinear optical properties of powder samples of $Cs_2CuP_3S_9$ using a pulsed Nd YAG laser were positive, judging from the frequency-doubled green light exiting the sample. Further work should be carried out to explore this property.

## ACKNOWLEDGMENT

## REFERENCES

1. (a) M. G. Kanatzidis, *Curr. Opinion Solid State Mater. Sci.* **2,** 139 (1997); (b) A. Sutorik and M. G. Kanatzidis, *Prog. Inorg. Chem.* **43,** 151 (1995).
2. T. J. McCarthy and M. G. Kantzidis, *Inorg. Chem.* **34,** 1257 (1995).
3. P. K. Dorhout and T. M. Malo, *Z. Anorg. Allg. Chem.* **622,** 385 (1996).
4. T. J. McCarthy and M. G. Kanatzidis, *Inorg. Chem.* **34,** 1257 (1995).
5. (a) J. H. Chen and P. K. Dorhout, *Inorg. Chem.* **34,** 5705 (1995); (b) J. H. Chen, P. K. Dorhout, and J. E. Ostenson, *Inorg. Chem.* **35,** 5627 (1996).
6. K. Chondroudis, T. J. McCarthy, and M. G. Kanatzidis, *Inorg. Chem.* **35,** 3451 (1996).
7. K. Chondroudis, J. A. Hanko, and M. G. Kanatzidis, *Inorg. Chem.* **36,** 2623 (1997).
8. J. A. Hanko, J. Sayettat, S. Jobic, R. Brec, and M. G. Kanatzidis, *Chem. Mater.* **10,** 3040 (1998).
9. K. Chondroudis and M. G. Kanatzidis, *Inorg. Chem.* **37,** 2848 (1998).
10. K. Chondroudis and M. G. Kanatzidis, *Inorg. Chem.* **37,** 2098 (1998).
11. V. Derstroff, V. Ksenofontov, P. Gutlich, and W. Tremel, *Chem. Commun.* 187 (1998).
12. V. Derstroff and W. Tremel, *Chem. Commun.* 913 (1998).
13. (a) $Cs_2CuP_3S_9$ was synthesized from a mixture of 0.032 g (0.50 mmol) Cu, 0.220 g (1 mmol) $P_2S_5$, and 0.149 g (0.50 mmol) $Cs_2S$ which was sealed under vacuum in a Pyrex tube and heated to 500°C for 4 days followed by cooling to 100°C at 4°C h$^{-1}$. The excess $Cs_x[P_yS_z]$ flux was removed by washing with degassed methanol under inert atmosphere to reveal irregular bright yellow crystals (75% yield based on Cu). Microprobe energy dispersive (EDS) analysis, on several ($>10$) single crystals, gave an average composition of $Cs_{2.22}CuP_{3.3}S_9$.
14. A Siemens SMART Platform CCD diffractometer from a crystal of $0.200 \times 0.200 \times 0.120$ mm dimensions and Mo$K\alpha$ ($\lambda = 0.71073$ Å) radiation. An empirical absorption correction was applied to the data during data processing. Crystal data at 23°C: $a = 15.874(2)$ Å; $b = 15.874(2)$ Å; $c = 35.100(7)$ Å; $\gamma = 120.00$; $V = 7660(3)$ Å$^3$; $Z = 18$; $D_{calc} = 2.767$ g/cm$^{-3}$; space group $P6_5$; $\mu = 6.804$ cm$^{-1}$ index ranges $-19 \le h \le 21$, $-20 \le k \le 21$, $-22 \le l \le 47$; total data 48681; unique data 9745; ($R_{int} = 0.0944$); data with $F_o^2 > 2\sigma(F_o^2)$ 4056; No. of variables, 406; final $R/R_w$ 0.030/0.069; GOF 0.335; largest diff. peak and hole $0.882/-0.767$ e Å$^{-3}$. (b) G. M. Sheldrick, "SHELXL: Version 5.03," Siemens Analytical X-ray Instruments, Inc., Madison, WI, 1994.
15. (a) Far-IR (CsI matrix) gave absorptions at 619(w), 519(w), 400(S), 463(s), 384(s), 370(s, sh), 241(w), and 161(w) cm$^{-1}$. (B) The Raman spectrum, in the same region, gave absorptions at 653(w, b), 586(m), 555(w), 486(w, b), 386(s), 325(m), 294(w), 254(w), 221(s) 175(m), and 150(w) cm$^{-1}$.
16. W. Brockner, R. Becker, B. Eisenmann, and H. Schaefer, *Z. Anorg. Allg. Chem.* **520,** 51 (1985).
17. O. Sala and M. L. A. Temperini, *Chem. Phys. Lett.* **36,** 625 (1975).